SAND2016-9880R

Advanced In-situ Diagnostics for Multicomponent Gas Analysis and Material Aging

David Robinson and Mark Allendorf
Sandia National Laboratories
Livermore, CA 94551

Part 1: Compact Sensing of Volatile Species

Abstract

Current methods of detecting material aging rely heavily on accelerated aging studies expensive, bulky, and resource-hungry diagnostics. We are developing compact gas analysis methods based on sensor platforms such as quartz crystal microbalances (QCM), using nanoporous metals and Metal-Organic Frameworks (MOFs), which enhance sensitivity and impart selectivity to analytes. Targeted analytes are O_2 and other volatile analytes. In FY16 we installed and tested a new QCM system coupled to a commercial gas mixing system. This instrumentation provides a new multi-use capability that: 1) allows evaluation of detection of novel materials to enable selective detection of volatile species relevant to Enhanced Surveillance; 2) accelerates development of new thin film deposition methods for depositing these materials on sensing devices; and 3) enables in-situ monitoring, with sub-monolayer sensitivity, of the interaction of volatile species with material surfaces subject to aging or corrosion.

Introduction

Current methods of detecting material aging rely heavily on accelerated aging studies, often employing gas analysis using gas chromatography and mass spectrometry. These diagnostics involve expensive, bulky, and resource-hungry instruments, and highly trained operators. Moreover, the correlation between gas analysis data from accelerated testing and corresponding data from actual stockpile measurements is unclear and lacks a basis in fundamental understanding. We are developing more compact gas analysis methods based on sensor platforms such as quartz crystal microbalances (QCM) and surface acoustic wave sensors (SAWS), which detect analytes by sensing mass change. We functionalize these devices with thin films of nanoporous materials known as Metal-Organic Frameworks (MOFs) to impart selectivity and reduce limits of detection. Currently, our devices are designed to detect one or a few chemically related analytes (e.g. water vapor and small alcohols). We believe that utility of these sensing concepts can be enhanced to detect a range of analytes, and simultaneously perform more than one function from among sensing, separation, and actuation, providing new paths to compact, versatile gas analysis methods. Moreover, our studies suggest that the versatility of devices such as the QCM extends beyond gas sensing. In particular, a QCM could be used to monitor material aging and compatibility phenomena by virtue of its ability to detect both sub-monolayer changes in mass and subtle alterations in mechanical properties. This would create a capability to rapidly screen materials to detect nascent aging or corrosion. Additionally, it could provide data useful for establishing correlations between long-term material tests and accelerated or laboratory material evaluations.

Approach

This part of the project takes advantage of a recently acquired quartz crystal microbalance (QCM) system that can monitor four different samples simultaneously, using a combination of fluid flow cells, electrochemical flow cells, and gas-uptake or humidity-controlled cells. This instrument will yield detailed information concerning the state of a thin-film sorbent sample as a function of gas environment and applied electrical current or potential. The microbalance measures the mechanical response of the film to very high-frequency vibrations, describing the added mass and changes in elastic modulus due to physi- or chemisorbed species.

We are considering the potential of Metal-Organic Frameworks invented by Allendorf (8300) and coworkers as multifunctional sorbent materials for imparting high sensitivity and selectivity to gases relevant to NW Enhanced Surveillance. The high surface-to-volume ratio in these materials, in which every atom is no more than a few atoms away from a surface, makes their physical properties, such as electrical conductivity, elastic modulus, and optical absorption, highly sensitive to adsorbates within their pores. Furthermore, we expect that the adsorptive properties can be electrically modulated, if only by ohmic heating. More complex architectures, such as a nanoporous film on a nonporous substrate, may lead to adsorption-induced strain effects or other effects that further couple electrical and surface properties. As part of this effort, we are using a new Quartz Crystal Microbalance (QCM) instrument and associated gas delivery equipment. MOFs will be grown as thin films on QCM substrates; their sorption properties will be measured using the new four-module QCM system. Target analytes will be oxygen (work initiated in FY15) and other volatile species. When combined with our previous demonstration of ultrahigh-sensitivity humidity detection using MOF-functionalized QCM and SAWS, this will enable simultaneous detection of gas constituents frequently associated with accelerated material aging.

Results and Impacts

<u>QCM-D Installation and Validation</u>

We purchased, setup, and validated a new QCM-D instrument (Biolin Scientific) that greatly enhances our abilities to measure the interactions of MOF sensors with small molecule analytes such as O_2 and H_2O. This instrument is capable of detecting sub-monolayer changes in mass and can used both gas sensing and for monitoring chemical reactions (such as corrosion) on surfaces. The new QCM is interfaced to a vacuum chamber and associated gas delivery system, described in detail below.

Figure 1 depicts the QCM liquid flow module setup, which is interfaced with a computer-controlled multiport valve (fabricated at Sandia). In this configuration, changes in mass resulting from surface reactions such as MOF film growth, the uptake of an analyte in solution, or the reaction of a corrosive medium with a material can be monitored in real time. A key innovation is the multiport valve we installed, which can be cycled between 8 inputs in synchronization with an on/off signal sent to a peristaltic pump downstream of the QCM flow module. This allows for a very fast (2 second) switch between flowing solutions, which minimizes bubble formation that is detrimental to a stable frequency measurement by the QCM sensor.

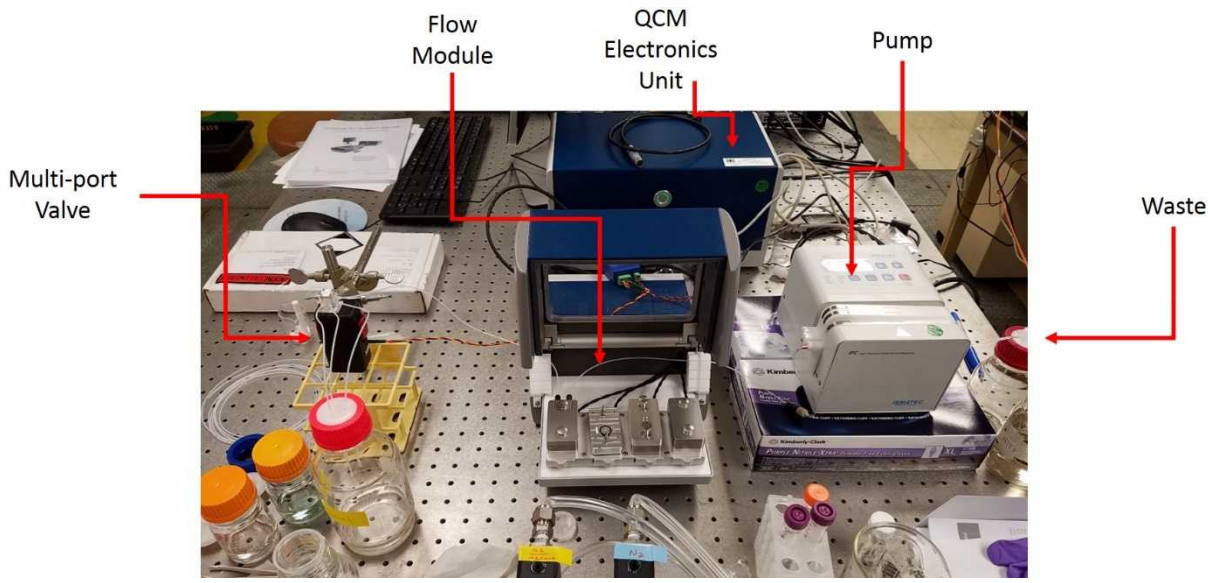

Figure 1. Biolin Scientific QCM-D flow-chamber setup with multiport valve.

We validated the QCM/valve setup by growing a film of the MOF HKUST-1 film, by standard methods we previously developed, on a COOH-terminated self-assembled monolayer (SAM). Ethanol solutions of 1 mM $Cu(OAc)_2$ and 0.2 mM trimesic acid were sequentially flowed over the QCM sensor with intermediate EtOH washes. The frequency changes data with respect to time are shown in Figure 2a. Also shown is the decay of higher harmonics of the QCM crystal, known as the dissipation, which provides an indication of the rigidity of the surface material (this feature can be used to make very accurate measurements of mechanical properties). The steady decrease in frequency corresponds to an increase in mass on the QCM surface, whereas the dissipation increase is related to the rigidity of the MOF surface layer. The initial increase in dissipation followed by a gradual decrease is likely due to an increase in crystallinity and film coverage as the film thickness increases. Figure 2b is an expanded view of the frequency data in Figure 2a, showing the self-limiting behavior (i.e., saturation of surface growth sites) during each layer-by-layer cycle. Since each growth cycle corresponds to uptake of only one component of the MOF structure (either the Cu(II) metal ion or the organic benzenetricarboxylate linker), it is clear that the device is readily sensitive to fractions of a monolayer in mass difference. The structure of the deposited film was verified as the MOF using grazing-incidence X-ray diffraction (Figure 3).

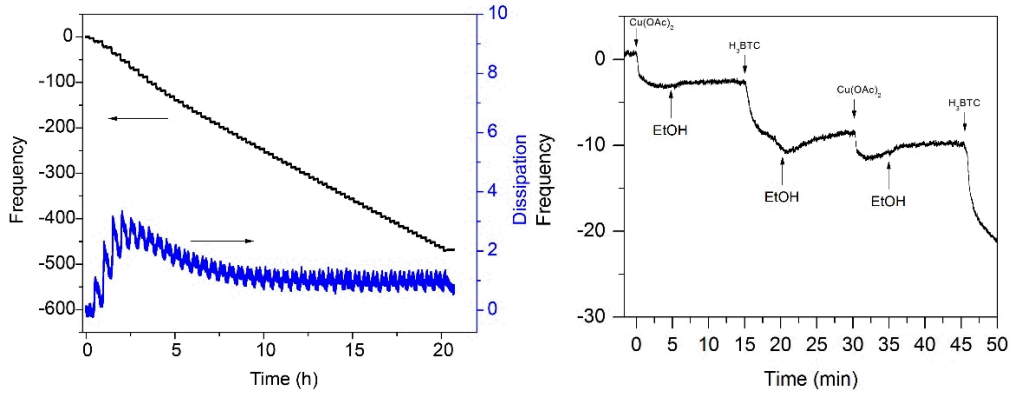

Figure 2. A) Frequency and dissipation data for 40 cycle of layer-by-layer HKUST-1 growth on an COOH terminated gold sensor. B) Frequency data for the first 2 layer-by-layer cycles with arrows indicated the flowing solutions at different time points.

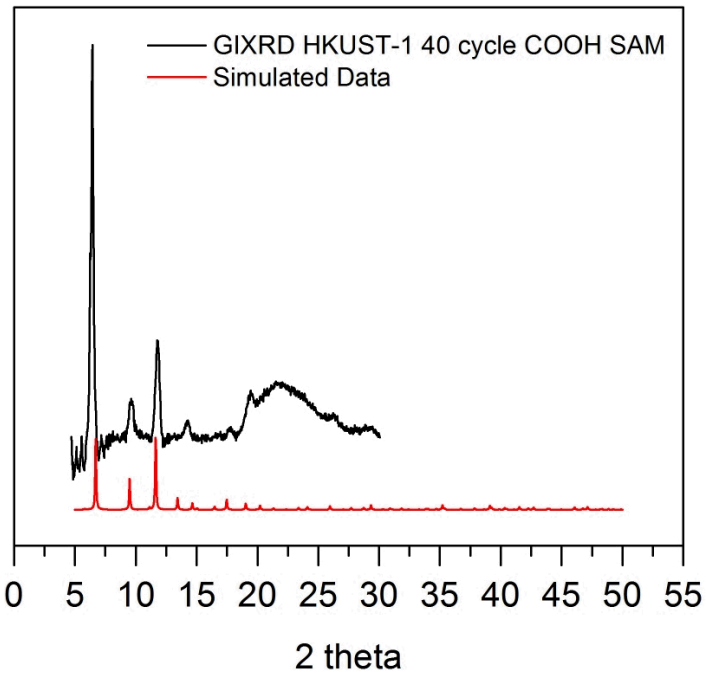

Figure 3. Comparison between GIXRD of LBL film and simulated powder pattern for HKUST-1.

In addition to the flow module, the QCM-D comes with an ALD sensor holder, which we have interfaced with a gas chamber and delivery system described below.

Vacuum chamber design and construction

We also designed and fabricated a small vacuum chamber for gas-phase sensing experiments to be performed using QCM sensors and a new vapor delivery system. This chamber allows “multi-axis” detection, in which changes in material optical properties are monitored through a glass window simultaneously with the mass uptake monitored by the QCM sensor. A residual gas analyzer (RGA) is also attached, which allows the composition of the atmosphere above the sample to be monitored in

real time. We are able to deliver specific quantities of gas mixtures via flow or stop-flow conditions using the attached Microtrac BELFlow gas delivery system. This system can deliver a dry or humid (0.02 - 95% relative humidity) mixture of two gases at flow rates between 1 and 100 sccm and can create a binary mixture from up to 10 attached gas sources. A schematic of the chamber is shown in Figure 4, with a photograph of the system shown in Figure 5.

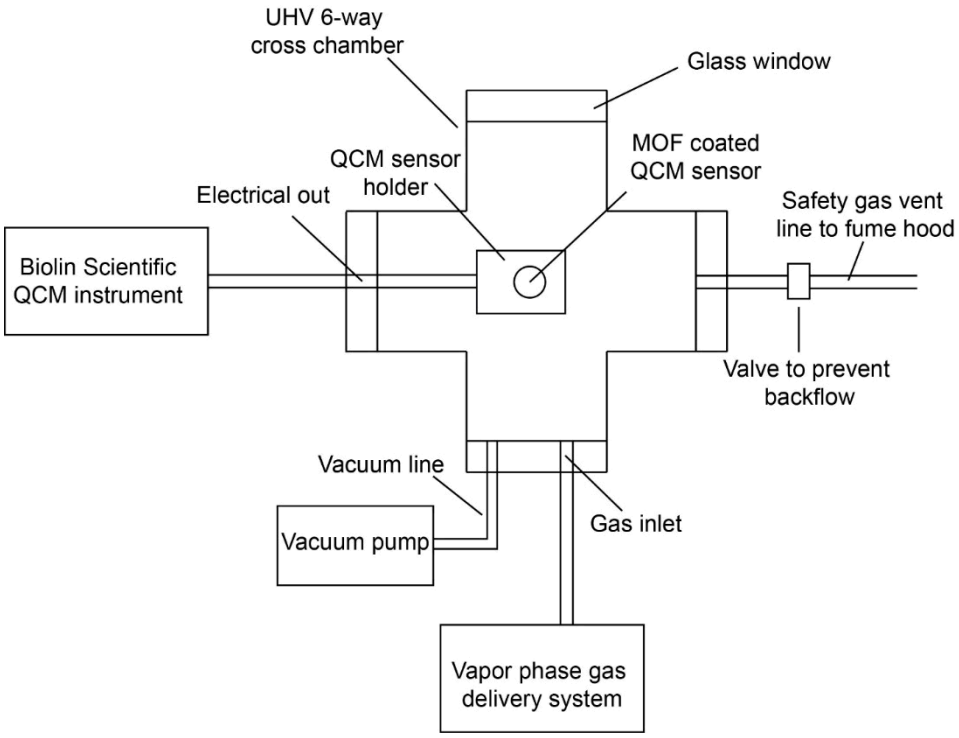

Figure 4. Design schematic of chamber for gas-phase sensing experiments.

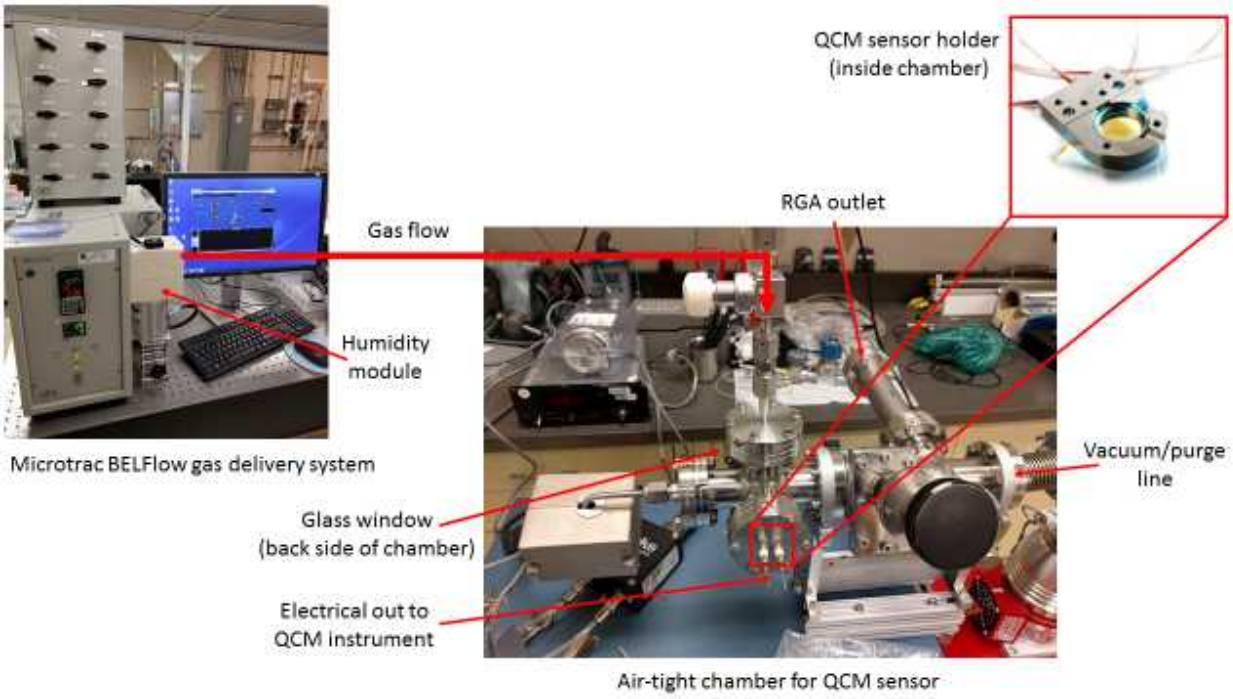

Figure 5. Microtrac BELFlow gas delivery system and air-tight chamber for QCM measurements

Conclusions and Future Work

In FY17 we will coat QCM surfaces with MOFs of varying thickness using solvothermal synthesis or layer-by-layer film growth, both of which are methods already developed by us. We will then conduct gas sensing experiments to identify and optimize MOFs for oxygen detection. Detection in both dry and humid atmospheres will be evaluated.

Advanced In-situ Diagnostics for Multicomponent Gas Analysis and Material Aging

Part 2: Compact Determination of Hydrogen Isotopes

David B. Robinson
Sandia National Laboratories
Livermore, CA 94551

Abstract

This report has been accepted for publication in the journal Fusion Science and Technology, in the special issue associated with the Tritium 2016 conference, where the work was presented.

Scanning calorimetry of a confined, reversible hydrogen sorbent material has been previously proposed as a method to determine compositions of unknown mixtures of diatomic hydrogen isotopologues and helium. Application of this concept could result in greater process knowledge during the handling of these gases. Previously published studies have focused on mixtures that do not include tritium. This paper focuses on modeling to predict the effect of tritium in mixtures of the isotopologues on a calorimetry scan. The model predicts that tritium can be measured with a sensitivity comparable to that observed for hydrogen-deuterium mixtures, and that under some conditions, it may be possible to determine the atomic fractions of all three isotopes in a gas mixture.

Introduction

Experimental studies of nuclear fusion often require the handling of mixtures of gaseous isotopologues of diatomic hydrogen, as well as helium isotopes that are products of fusion or the decay of tritium. A prevalent method to determine compositions of these mixtures involves leaking a small quantity of the gas into a vacuum chamber, ionizing it, and performing mass spectrometry. A low-cost quadrupole mass spectrometer has typical detection limits for a given species of a few tenths of a percent; more expensive instruments such as magnetic sector mass spectrometers have lower limits. However, mass spectrometers and their vacuum hardware are generally bulky and consume large amounts of energy. When tritium is used, that bulky hardware becomes contaminated. The vacuum pumps produce undesirable waste streams of dilute tritium in their exhaust, and replacement of worn pump parts produces additional tritium-contaminated waste. Especially when tritium is used, it would be valuable to have methods to measure composition that do not require a vacuum system.

A previous publication proposed a method to determine composition using scanning calorimetry of a reversible hydrogen-absorbing material in a small capsule with a laser-drilled hole.[1] Experiments with hydrogen, deuterium, and helium-4, using palladium as the hydrogen-absorbing material, demonstrated that mixtures of about 1% of one gas in another yield calorimetry scans that are distinguishable from those of the pure gases. The pure hydrogen isotopes absorb into (and desorb from) the palladium at temperatures differing by tens of degrees C, with mixtures absorbing at intermediate temperatures. Helium modifies the absorption and desorption by forming a temporary blanket of helium-rich,

hydrogen isotope-poor gas in the capsule during absorption, and a helium-poor, hydrogen isotope-rich gas during desorption. This results in an increased separation of the absorption and desorption peaks, with characteristic peak shapes, aiding deduction of the helium mole fraction. This effect is not predicted to be strongly dependent on the isotopic composition of the helium. A model accounting for mass transport and the thermodynamics and kinetics of absorption predicts the positions and shapes of the calorimetry peaks. Experiments with tritium have not been performed, and the model was not applied to these in the previous work. In this report, the model is extended to account for tritium, and its predictions are evaluated for mixtures of two or three hydrogen isotopes. The effect of helium in the presence of tritium is not expected to differ significantly from the effect of helium on the other hydrogen isotopes as described in Ref. 1, so for brevity, helium is not considered here.

Approach

In the scenario to be modeled, a mixture of $^{1}H_2$, $^{2}H_2$, $^{3}H_2$ is present in and around a capsule containing a small amount of palladium, as in the experimental geometry described in Ref. 1. The choice of palladium is motivated by its ability to reversibly absorb and desorb hydrogen near room temperature and atmospheric pressure; its robustness against surface fouling and bulk oxidation, which make it convenient to handle in laboratory conditions; and the existence of literature data on the equilibrium amounts of each hydrogen isotope in the solid as a function of temperature and pressure. It is assumed that the mixed hydrogen isotopologues such as $^{1}H^{2}H$ exist in their equilibrium amounts, and have an effect on the solid-gas equilibrium. Enthalpies of formation of the mixed isotopologues are typically less than 1 kJ/mol, which is similar to the reported uncertainties in the enthalpies of absorption of hydrogen isotopes into palladium, so the chemical effects of the mixed isotopologues are relatively minor.[2,3] Similarly, it is assumed that the effects of the mixed isotopologues on the physical properties of the gas (viscosity, heat capacity, diffusion coefficient) are within the uncertainty related to other approximations in the transport model, so that the mass transport equations treat all gas-phase ^{1}H as existing as $^{1}H_2$, etc.

Fig. 1 presents a graphical representation of the capsule geometry, gas concentrations, and hydride-to-metal ratios accounted for by the transport model. Table 1 describes other transport model parameters.

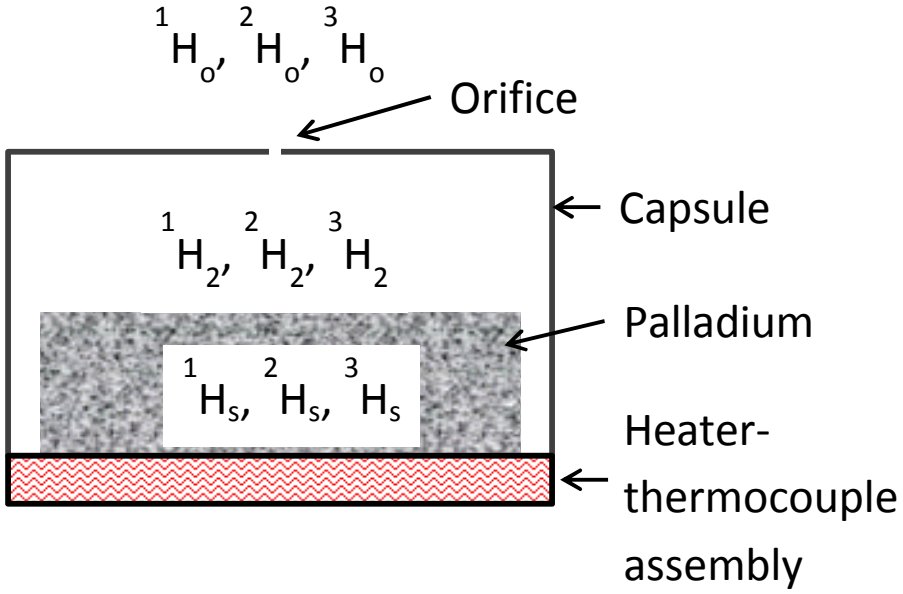

Fig. 1. The calorimetry model accounts for constant external gas concentrations ^iH_o, variable concentrations $^iH_2$ inside the capsule, and variable solid-phase hydride-to-metal ratios ^iH_s (i = 1, 2, or 3).

Table 1. Parameters in transport model.

$^iH_{eq}$	Value of $^iH_2$ that would be at equilibrium with the solid composition (mol/m^3)
n_o	Sum over i of ^iH_o (mol/m^3)
n	Sum over i of $^iH_2$ (mol/m^3)
T_o	External temperature (K)
T	Temperature inside the capsule (K; reported as °C in figures)
R	Ideal gas constant (J/mol K)
r	Radius of orifice that allows gas transport in and out of capsule (m)
L	Length of capsule orifice (m)
V	Volume of capsule (m^3)
m	Moles of palladium
μ	Gas viscosity (Pa s)
D_i	Diffusion coefficient of gas species i (m^2/s)
k	Rate constant for absorption and desorption (m^3 mol^{-1} s^{-1})
t	Time (s)

Gas transport is described in the model by a set of equations that each account for pressure-driven flow through the orifice, diffusion through the orifice, and absorption/desorption into the solid. The flow term is treated as laminar flow through a pipe, as a simple hypothesis for its dependence on

orifice geometry and pressure. The diffusion term uses a one-dimensional model. The absorption/desorption rate is assumed to be linearly proportional to the concentration difference from the equilibrium state, as determined below. Because the composition of flowing gas depends on the flow direction, the transport equations take two different forms. When the first term is positive ($n_oRT_o > nRT$), gas flows into the capsule, with the composition of the external gas:

$$V\frac{d^iH_2}{dt}=\frac{\pi r^4}{8\mu L}\frac{^iH_o}{n_o}\left(n_oRT_o-nRT\right)+\frac{D\pi r^2}{L}\left(^iH_o-^iH_2\right)-km\left(^iH_2-^iH_{eq}\right) \quad (1)$$

When the first term is negative, gas flows out of the capsule, and the flowing gas has the same composition as the gas within the capsule:

$$V\frac{d^iH_2}{dt}=\frac{\pi r^4}{8\mu L}\frac{^iH_2}{n_o}\left(n_oRT_o-nRT\right)+\frac{D\pi r^2}{L}\left(^iH_o-^iH_2\right)-km\left(^iH_2-^iH_{eq}\right) \quad (2)$$

The viscosity (Ref. 4) and diffusion (Ref. 5) coefficients were taken as an average of literature values weighted by ^iH_o, and incorporated the temperature dependence of viscosity (Ref. 6) and pressure dependence of diffusion coefficient (Ref. 5) from the literature. Transport of each solid-phase hydride species ^iH_s is given by

$$m\frac{d^iH_s}{dt}=2km\left(^iH_2-^iH_{eq}\right) \quad (3)$$

where the factor of two accounts for dissociation of the diatomic gas molecules. The main case of interest in this work is where transport between solid and gas is fast, and the solid-gas system is near equilibrium. The value of k in this work was chosen to be large enough that model predictions are insensitive to k, indicating that the solid-gas system is near equilibrium, but small enough to ensure convergence during simulation. In effect, this makes gas transport through the orifice the rate-limiting step in an overall absorption or desorption process. Use of a small k value results in peak broadening that can obscure some of the results described in this work.

Values of $^iH_{eq}$ were obtained by literature procedures that consider that the chemical potentials between the gas and solid phase are equal under equilibrium conditions.[1,7,8] The parameters in the solid-gas equilibrium model are described in Table 2.

Table 2. Parameters in solid-gas equilibrium model.

H_s	Sum over i of ^iH_s
P_{ij}	Partial pressure of diatomic gas species $^iH_s{}^jH_s$ (Pa)
μ_i^0	Standard-state chemical potential of solid hydride species ^iH_s (mol/m^3)
μ_{ij}^0	Standard-state chemical potential of diatomic gas species $^iH_s{}^jH_s$ (mol/m^3)
μ^{ex}	Excess chemical potential (a function of H_s) (mol/m^3)

The partial pressures of the diatomic gas species (including the mixed isotopologues) are obtained from the chemical potentials by

$$RT\ln\left(P_{ij}/1\text{ atm}\right)=\left(\mu_i^0+\mu_j^0-\mu_{ij}^0\right)+RT\ln\left(\frac{{}^iH_s\cdot{}^jH_s}{1-H_s}\right)+2\mu^{ex} \quad (4)$$

where the standard-state chemical potentials depend only on temperature and species identity as described in Refs. 1 and 9. The second term captures the entropy of mixing in the solid. The excess chemical potential term captures nonideal chemical effects at high concentrations, depends only on *H*, and is described as a polynomial empirical fit in Refs. 1 and 10. Equation 4 does not account for the phase transition between the dilute (alpha) and concentrated (beta) phases of palladium hydride, during which the gas pressure is constant over a wide temperature range. The transition pressures were empirically correlated to the minima in Equation 4 as described in Ref. 1, and the partial pressures constrained to be monotonic functions that have values lower than the transition pressure at low *H*, and higher than the transition pressure at high *H*. Absorption and desorption each have a different transition pressure due to the work required to rearrange metal atoms during the phase transition; the system departs from equilibrium when these processes are underway.

Because the mixed gas-phase isotopologues are not accounted for in the transport equations, their atoms are treated as rearranged into single-isotope diatomic species:

$${}^iH_{eq}=\frac{P_{ii}}{2RT}+\sum_j\frac{P_{ij}}{2RT} \quad (5)$$

Heat flow was computed as described in Ref. 1. The main components of the heat flow are the reaction enthalpies of absorption or desorption for each isotope (obtained from Refs. 1, 3, and 9), multiplied by d^iH_s/dt. To obtain an enthalpy for tritium absorption based on Ref. 3, which only reports a value for desorption, it was assumed that the hysteresis for tritium is about the same as the other isotopes. Additional components are included to account for the heat capacity of the sorbent, capsule, and incoming gas. The model equations were solved using the implementation of LSODE (Livermore Solver for Ordinary Differential Equations) in GNU Octave.[11]

Results and Impacts

The solid-gas equilibrium model can be checked separately from the transport model by using it to predict the results of pressure-composition isotherm experiments, and comparing to previously published results. Figure 2 shows the predictions for each pure isotope at a variety of temperatures. The isotherms show the expected behavior where the transition region is between about 0 and 0.6 hydrogens per Pd atom (H/Pd) at lower temperatures, narrowing at higher temperatures, and reaching a critical point near 300 °C and several tens of atm (Ref. 12). At 100 °C, the transition pressure ratio for deuterium:hydrogen is about 3.4; 1.7 for tritium:deuterium, and 5.8 for tritium:hydrogen, increasing at

lower temperatures and decreasing at higher temperatures. These ratios are about the same as for previously reported experimental desorption curves at 90 °C (Ref. 13). The absolute pressures also closely match, after accounting for the temperature dependence reported in Ref. 13. Other factors such as gas purity (Ref. 13) and the effect of sample form on the amount of hysteresis (Ref. 1) can introduce variation between published reports. Examples of pressure-composition isotherms for a $^{1}H_2$-$^{2}H_2$ mixture are discussed in Ref. 1.

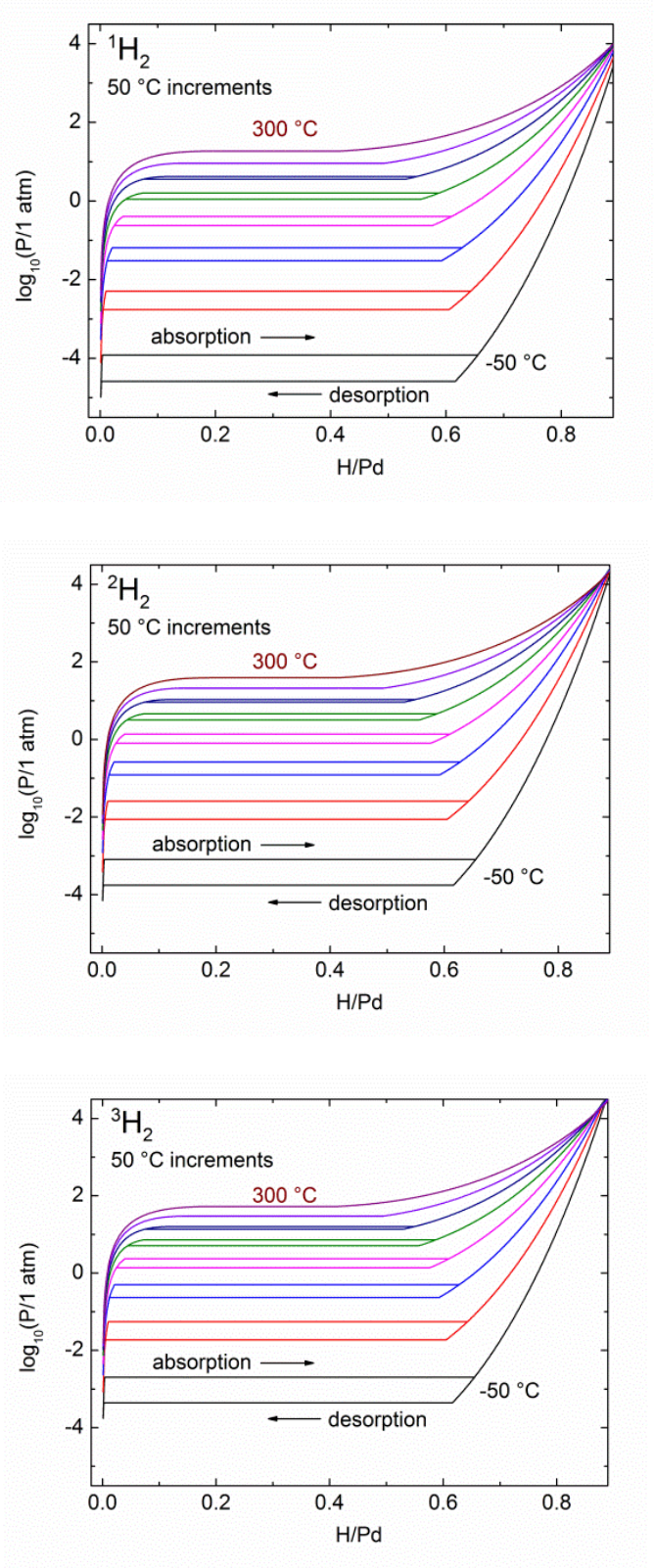

Fig. 2. Predicted pressure-composition isotherms for each pure hydrogen isotope at 50 °C intervals between -50 and 300 °C.

In a simulated experiment described in Ref. 1, a series of calorimetry scans is performed, where the total pressure is held constant, but the ratio of $^1H_2$ to $^2H_2$ is varied for different scans. This provides a succinct summary of many predictions of the transport model under these conditions. Figure 3 shows sets of simulated scans for both the $^1H_2$ - $^2H_2$ pair and the $^2H_2$ - $^3H_2$ pair. The pure gases show relatively sharp peaks. The mixtures show broader peaks at temperatures between those of the pure gases. The broadest peaks occur at temperatures about halfway between the pure-gas peaks. For absorption, the broadest peaks are near a 1:1 gas-phase mixture, whereas for desorption (as can be observed from other simulation variables) the broadest peaks are near a 1:1 solid-phase mixture. The breadth is caused mainly by the mass transport restriction of the orifice, which causes temporary variations in composition within the capsule, as described in Ref. 1.

Just as the pure-gas pressure ratio for $^3H_2$:$^2H_2$ is smaller than for $^2H_2$:$^1H_2$, the temperature difference between their calorimetry peaks is smaller, providing a narrower range in which to determine composition of gas mixtures using peak position. However, the peak widths are not as broad, so the ability to measure small differences in composition, or small fractions of one component in another, is not severely degraded.

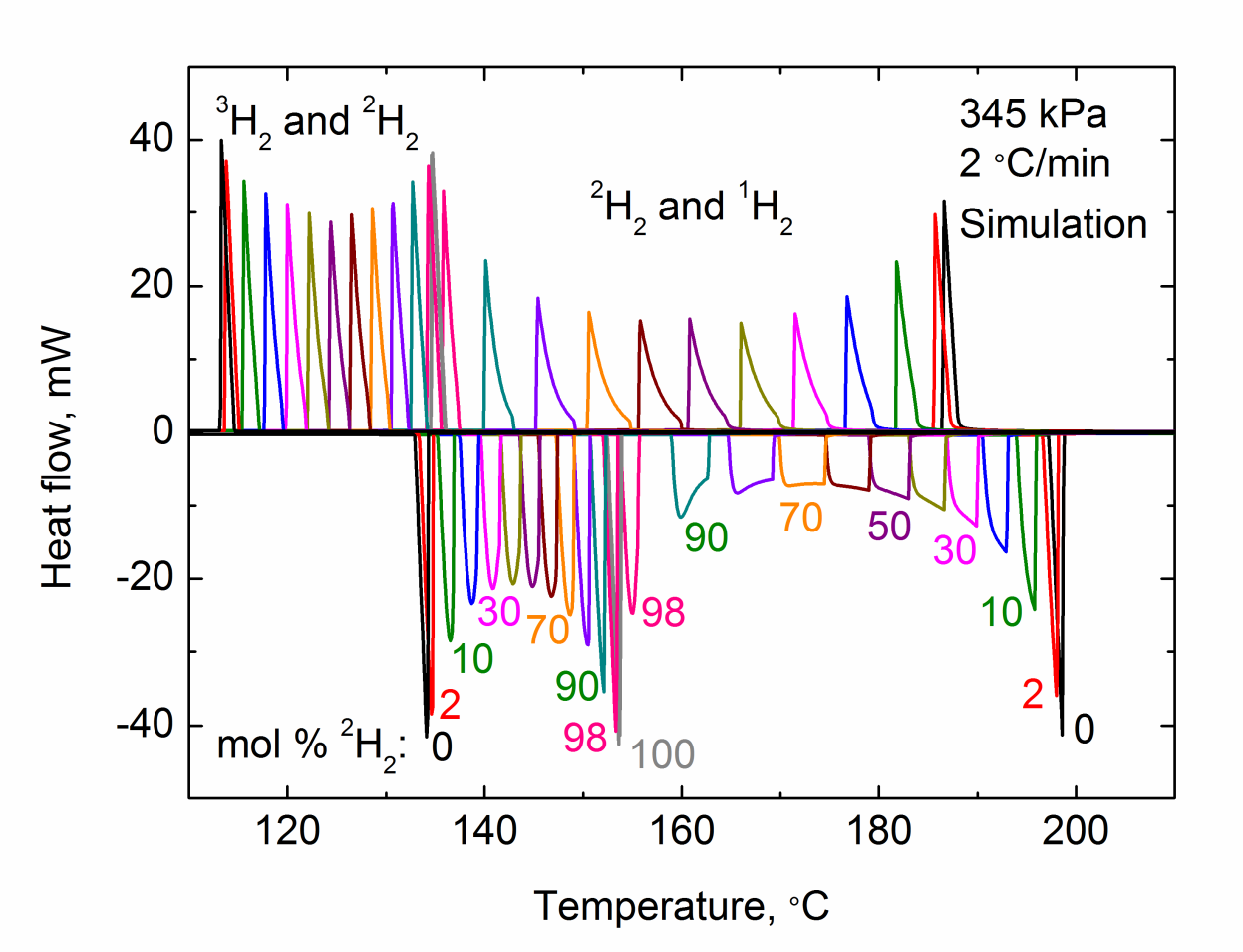

Fig. 3. Simulated calorimetry scans at a constant total pressure, but varying amounts of $^2H_2$ mixed with either $^1H_2$ or $^3H_2$ in the gas phase. Negative heat flows correspond to desorption, and positive heat flows correspond to absorption.

The case of $^1H_2$ - $^3H_2$ is shown in Figure 4. The pure-gas peaks are well separated on the temperature axis. As compared to the $^1H_2$ - $^2H_2$ case, peaks at intermediate compositions show greater broadening. Adding a small amount of $^1H_2$ to pure $^3H_2$ causes a larger peak shift, whereas adding a small amount of $^3H_2$ to pure $^1H_2$ has an effect similar to adding a small amount of $^2H_2$. The broadest peak in Figure 4 occurs at 20% $^1H_2$, as opposed to 30% for the $^1H_2$ - $^2H_2$ mixtures in Figure 3.

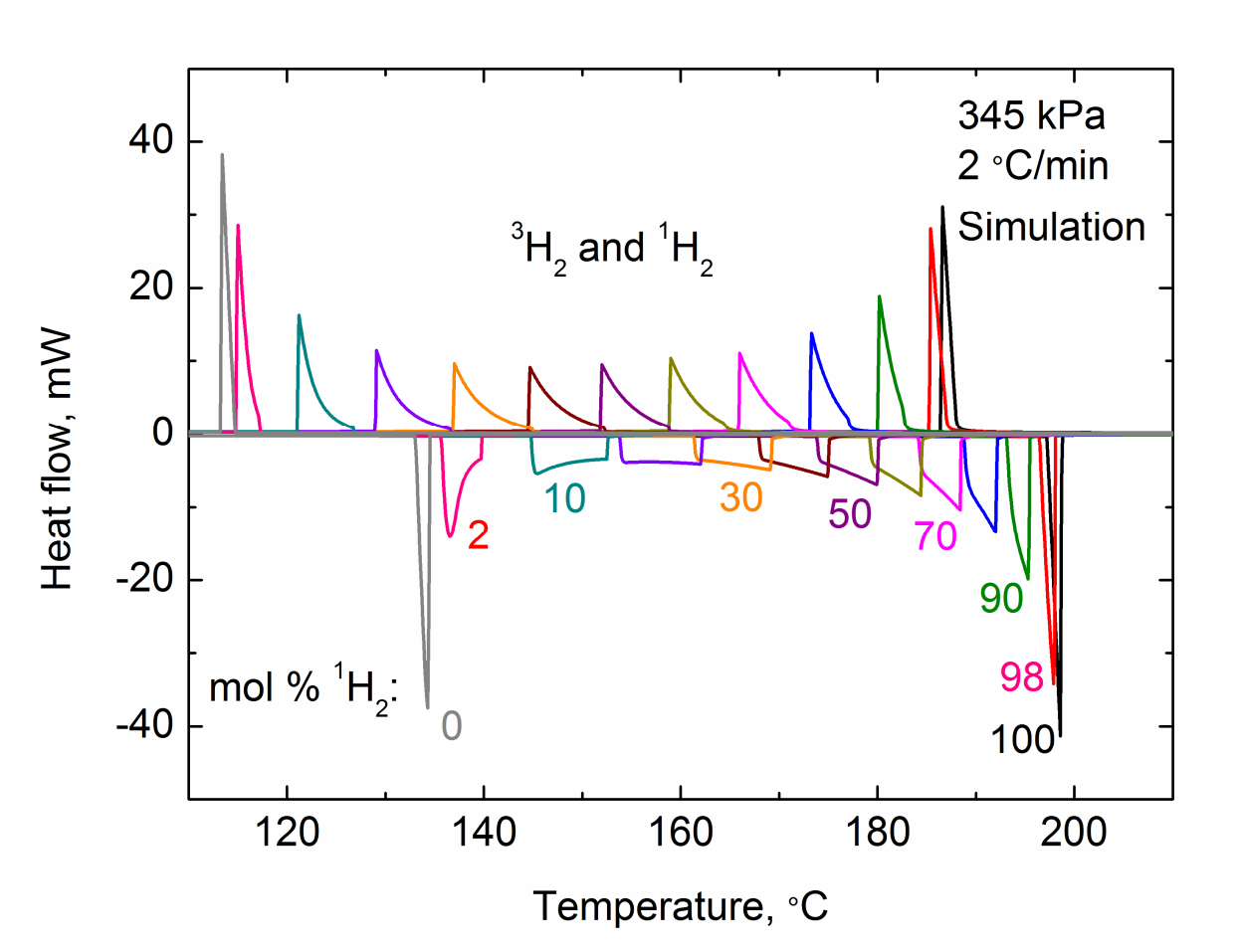

Fig. 4. Simulated calorimetry scans at a constant total pressure, but varying amounts of $^1H_2$ mixed with $^3H_2$ in the gas phase. Negative heat flows correspond to desorption, and positive heat flows correspond to absorption.

The previous results suggest that if a gas mixture contains only two known hydrogen isotopes, and the total pressure is known, the mole fractions of each isotope could be determined from a calorimetry experiment to within 2% of the total mixture. If the identity of the isotopes is not known, there is usually more than one pair of isotopes that could result in a measured peak position, but it should still be possible to identify the pair based on peak shape, as long as there is a significant amount of each isotope (at least 10%).

In fact, the peak shape may also allow identification of ternary mixtures in some cases. Figure 5 shows an example where the relative amounts of a $^1H_2$ - $^3H_2$ mixture (of a fixed ratio) and $^2H_2$, each of which yield peak onsets at approximately the same temperature, are varied. The $^1H_2$ - $^3H_2$ mixture alone produces broad peaks, whereas pure $^2H_2$ produces narrow peaks, and intermediate compositions result in a gradual transition from one peak shape to the other. With further elaboration, it may be possible to identify a range of ternary compositions that yield unique, measurable combinations of peak position and shape that would allow their determination from unknown mixtures by calorimetry.

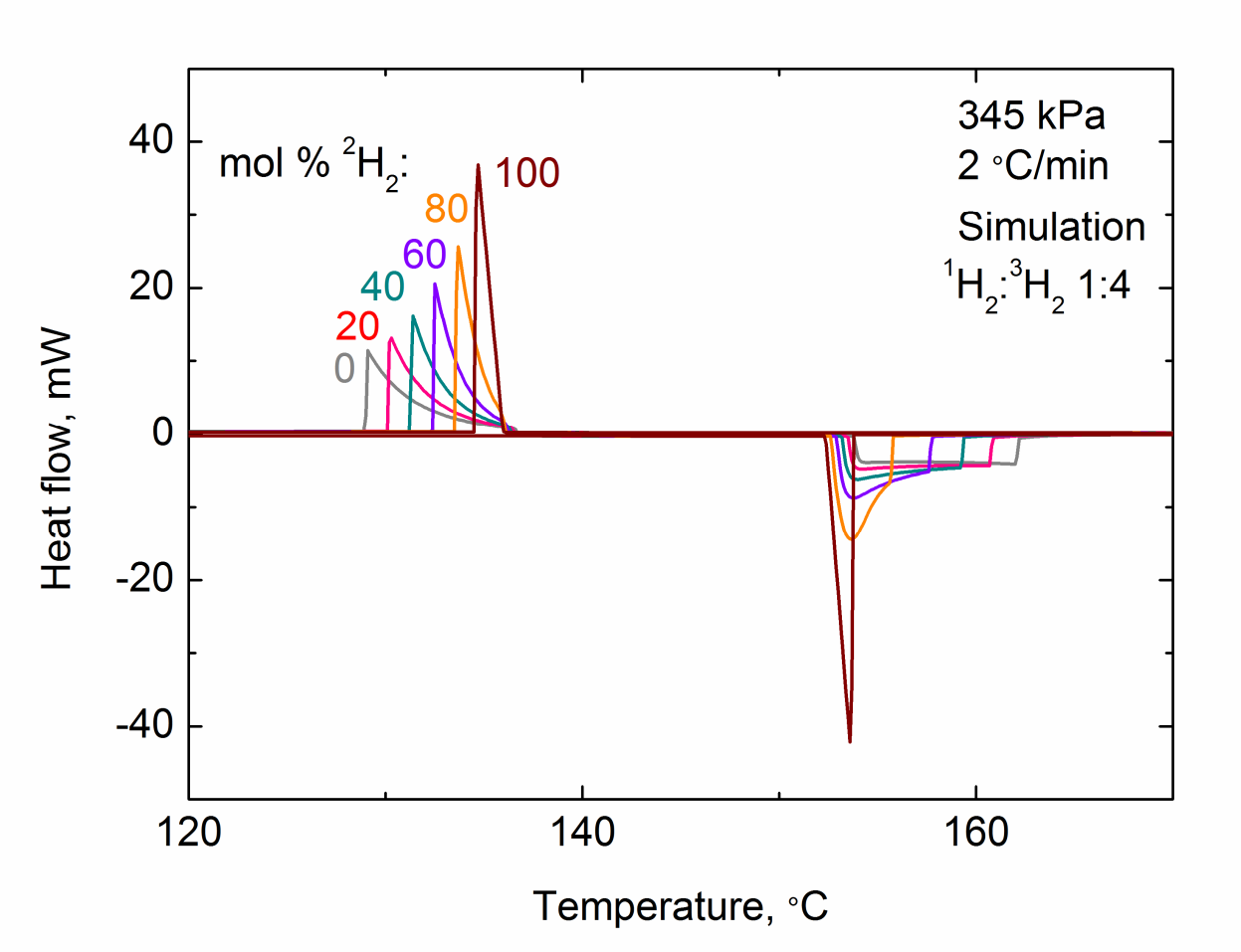

Fig. 5. Simulation of calorimetry scans on a series of gas mixtures starting with a 1:4 mixture of $^1H_2$:$^3H_2$, then adding a dose of $^2H_2$, and venting to maintain constant pressure between each scan.

Conclusions and Future Work

The calorimetry model described in Ref. 1 has been extended to account for tritium. The model predicts results for $^1H_2$ - $^3H_2$ and $^2H_2$ - $^3H_2$ mixtures that are qualitatively similar to the prior predictions for $^1H_2$ - $^2H_2$ mixtures, but quantitatively unique enough in most cases to allow the isotopic pair of a binary mixture to be identified. The simulations suggest that it may be possible to uniquely quantify some compositions containing all three hydrogen isotopes. Detection limits of small quantities of tritium in another isotope, or small quantities of another isotope in tritium, are close to those described in Ref. 1 for $^1H_2$ and $^2H_2$. As described in Ref. 1, if helium were also present, the ability to identify and quantify the hydrogen components of a mixture would be compromised to a degree dependent on the helium mole fraction, because the helium imposes peak broadening that could obscure the peak shapes of the hydrogen isotope mixtures. The model presented here does not make detailed consideration of all effects that might limit response time and peak resolution, such as the heat capacity of the heating and sensing elements, slow equilibration between the gas and solid, or noise in the system. Therefore, calorimetry offers the ability to provide useful information about the composition of a gas mixture,

although there are some regions of pressure, composition, and temperature space that provide more information than others, or that provide information more quickly. This can be compared to the challenge in mass spectrometry of distinguishing $^{2}H_{2}$, $^{1}H^{3}H$, and ^{4}He; each technique has its advantages and limitations. It can be expected that the combination of calorimetry and mass spectrometry would provide a more complete description of the composition of these light gas mixtures, and allow for a reduced dependence on mass spectrometry alone. This could lead to improved system knowledge and safety, as well as reduced costs, in processes that handle tritium.

Acknowledgement

Sandia National Laboratories is a multi-mission laboratory managed and operated by Sandia Corporation, a wholly owned subsidiary of Lockheed Martin Corporation, for the United States Department of Energy's National Nuclear Security Administration under contract DE-AC04-94AL85000.

Summary of Findings and Capabilities Related to Aging

No findings relevant to specific component/material aging or capabilities were obtained this year.

Related Publications, Presentations, and patents:

Stavila, V., Schneider, C., Mowry, C., Zeitler, T. R., Greathouse, J. A., Robinson, A. L., Denning, J. M., Volponi, J., Leong, K., Quan, W., Tu, M., Fischer, R. A., Allendorf, M. D. "Thin Film Growth of nbo MOFs and their Integration with Electroacoustic Devices," *Adv. Funct. Mater.*, **26** (2016), 1699 **Cover feature**.

"Colorometric Detection of Water Using MOF-Polymer Films and Composites," U.S. Patent 9,347,923 M. D. Allendorf, A. A. Talin.

D. B. Robinson, W. Luo, T. Y. Cai, and K. D. Stewart. "Metal Hydride Differential Scanning Calorimetry as an Approach to Compositional Determination of Mixtures of Hydrogen Isotopes and Helium." Int. J. Hydrogen Energy, Volume 40, Issue 41, 2 November 2015 (accepted August 2015), Pages 14257–14270. http://dx.doi.org/10.1016/j.ijhydene.2015.08.033

D. B. Robinson, "Compact Determination of Hydrogen Isotopes", Fusion Sci. Tech., accepted August 2016. http://dx.doi.org/10.13182/FST16-197 (not yet available online as of the report submission date).

Milestone Status:

1. **Initial QCM tests of nanoporous metal and conducting MOF films in air and O_2 (planned completion date: 12/31/2015).** Status: Due to delayed arrival of the new QCM and gas delivery systems, we were unable to complete this milestone. As of the date of this report, the equipment is now in place to conduct these experiments, which we project will be completed by 3/31/2017.
2. **QCM measurements of sorbents response to trace analytes in inert gas (planned completion date: 3/31/2016).** For the reasons stated under Milestone (1) above, we were unable to complete this milestone. We project that these experiments will be completed by 8/31/2017.
3. **Modeling.** The modeling work presented in Part 2 was not among our initial milestones proposed in late FY15, but was identified as a valuable extension of our FY15 work, and was discussed with the Sandia program manager upon the changing circumstances described in Milestone 1 and a 6-month acting management assignment to Robinson in the first half of the year.

References

[1] D. B. ROBINSON, W. LUO, T. Y. CAI, K. D. STEWART, "Metal Hydride Differential Scanning Calorimetry as an Approach to Compositional Determination of Mixtures of Hydrogen Isotopologues and Helium," *Int. J. Hydrogen Energy*, **40**, 14257 (2015).

[2] G. W. FOLTZ, C. F. MELIUS, "Studies of isotopic exchange between gaseous hydrogen and palladium hydride powder," *J. Catalysis*, **108**, 409 (1987).

[3] R. LÄSSER, K.-H. KLATT, "Solubility of hydrogen isotopes in palladium," *Phys. Rev. B*, **28**, 748 (1983).

[4] F. P. INCROPERA, D. P. DEWITT, T. L. BERGMAN, A. L. LAVINE, "Fundamentals of Heat and Mass Transfer," Wiley Interscience, 2007. ISBN: 978-0-470-91323-9

[5] R. B. BIRD, W. E. STEWART, E. N. LIGHTFOOT, "Transport Phenomena," 2nd ed., Wiley, 2002. ISBN: 978-0-470-50863-3

[6] F. M. WHITE, "Viscous Fluid Flow," 3rd ed., McGraw-Hill, New York, NY, 2006. ISBN: 978-0072402315

[7] W. A. OATES, R. LÄSSER, T. KUJI, T. B. FLANAGAN, "The effect of isotopic substitution on the thermodynamic properties of palladium-hydrogen alloys," *J. Phys. Chem. Solids* **47**, 429 (1986).

[8] W. G. WOLFER, B. A. MEYER, K. J. FISHER, "The vibrational, elastic and electronic contributions to the chemical potentials of hydrogen isotopes in palladium," in: N.R. Moody, A.W. Thompson, R.E. Ricker, G.S. Was, R.H. Jones, editors, Hydrogen Effects on Material Behavior and Corrosion Deformation Interactions. International Conference on Hydrogen Effects on Material Behavior and Corrosion Deformation Interactions; 2002 Sep 22-26; Moran, WY. Warrendale, PA: Minerals, Metals and Materials Society; 2003, p. 107-16.

[9] R. LÄSSER, G. L. POWELL, "Solubility of H, D, and T in Pd at low concentrations," *Phys. Rev. B* **34**, 578 (1986).

[10] T. B. FLANAGAN, T. KUJI, W. A. OATES, "The effect of isotopic substitution on the α-α' phase transition in metal-hydrogen systems," *J. Phys. F* **15**, 2273 (1985).

[11] J. W. EATON et al., "GNU Octave," http://www.octave.org

[12] F. A. LEWIS, "Palladium-Hydrogen System: Structures near phase transition and critical points," *Platinum Metals Rev.* **38**, 3, 112 (1994).

[13] R. LÄSSER, "Palladium-tritium system," *Phys. Rev. B.* **26**, 6, 3517 (1982).